Bachan, L., Storm, C. B., Wheeler, J. W., & Kaufman, S. (1974) *J. Am. Chem. Soc. 96*, 6799-6800.
Bell, R. P. (1973) *The Proton in Chemistry*, 2nd ed., Cornell University Press, Ithaca, NY.
Chatelus, G. (1964) *Bull. Soc. Chim. Fr. 10*, 2523-2532.
Clement, G. E., & Potter, R. (1971) *J. Chem. Educ. 48*, 695-696.
Craig, H. (1961) *Science (Washington, D.C.) 133*, 1702-1703.
Dahlquist, F. W., Rand-Meier, T., & Raftery, M. A. (1969) *Biochemistry 8*, 4214-4221.
Friedman, I. (1963) *Trans., Am. Geophys. Union 44*, 521-523.
Friedman, I., O'Neil, J. R., Adami, L. H., Gleason, J. D., & Hardcastle, K. (1970) *Science (Washington, D.C.) 167*, 538-540.
Hartley, P. E. (1980) *Anal. Chem. 52*, 2232.
Hermes, J. D., Roeske, C. A., O'Leary, M. H., & Cleland, W. W. (1982) *Biochemistry 21*, 5106-5114.
Ho, T.-L., Ho, H. C., & Wong, C. M. (1972) *J. Chem. Soc., Chem. Commun.*, 791.
Karoum, F., Cattabeni, F., Costa, E., Ruthven, C. R. J., & Sandler, M. (1972) *Anal. Biochem. 47*, 550-561.
Kishima, N., & Sakai, H. (1980) *Anal. Chem. 52*, 356-358.
Klinman, J. P. (1972) *J. Biol. Chem. 247*, 7977-7987.
Klinman, J. P., & Krueger, M. (1982) *Biochemistry 21*, 67-75.
Klinman, J. P., Humphries, H., & Voet, J. G. (1977) *Fed. Proc., Fed. Am. Soc. Exp. Biol. 36*, 2082.
Klinman, J. P., Humphries, H., & Voet, J. G. (1980) *J. Biol. Chem. 255*, 11648-11651.
Nageswara Rao, B. D., Kayne, F. J., & Cohn, M. (1979) *J. Biol. Chem. 254*, 2689-2696.
Niederl, J. B., & Ziering, A. (1942) *J. Am. Chem. Soc. 64*, 885-886.
Northrop, D. B. (1975) *Biochemistry 14*, 2644-2651.
Northrop, D. B. (1977) in *Isotope Effects in Enzyme-Catalyzed Reactions* (Cleland, W. W., O'Leary, M. H., & Northrop, D. B., Eds.) pp 122-152, University Park Press, Baltimore, MD.
Seebach, D., Erickson, B. W., & Singh, G. (1966) *J. Org. Chem. 31*, 4303-4304.
Swain, C. G., Stivers, E. C., Reuwer, J. F., Jr., & Schaad, L. J. (1958) *J. Am. Chem. Soc. 80*, 5885-5893.

Mechanism of Modulation of Dopamine β-Monooxygenase by pH and Fumarate As Deduced from Initial Rate and Primary Deuterium Isotope Effect Studies†

Natalie Ahn and Judith P. Klinman*

ABSTRACT: Dopamine β-monooxygenase catalyzes a reaction in which 2 mol of protons are consumed for each turnover of substrate. Studies of the pH dependence of initial rate parameters (V_{max} and V_{max}/K_m) and their primary hydrogen isotope effects show that at least two ionizable residues are involved in catalysis. One residue (B1, pK = 5.6-5.8) must be protonated prior to the carbon-hydrogen bond cleavage step, implying a role for general-acid catalysis in substrate activation. A second protonated residue (B2, pK = 5.2-5.4) facilitates, but is not required for, product release. Recent measurement of the intrinsic isotope effect for dopamine β-monooxygenase [Miller, S. M., & Klinman, J. P. (1983) *Biochemistry* (preceding paper in this issue)] allows an analysis of the pH dependence of rate constant ratios and in selected instances individual rate constants. We demonstrate large changes in the rate-determining step as well as an unprecedented inversion in the kinetic order of substrate release from ternary complex over an interval of 2 pH units. Previously, fumarate has been used in dopamine β-monooxygenase assays because of its property of enzyme activation. Studies of the pH behavior in the presence of saturating concentrations of fumarate have shown two causes of the activation: (i) fumarate perturbs the pK of B1 to pK = 6.6-6.8 such that the residue remains protonated and the enzyme optimally active over a wider pH range; (ii) fumarate decreases the rate of dopamine release from the ternary enzyme–substrate complex, increasing the equilibrium association constant for dopamine binding. Both effects are consistent with a simple electrostatic stabilization of bound cationic charges by the dianionic form of fumarate.

Dopamine β-monooxygenase is a copper containing monooxygenase catalyzing the hydroxylation of a variety of substituted phenylethylamines at their benzylic positions. These reactions involve a two-electron reductive cleavage of dioxygen via a poorly understood interaction of dioxygen with enzyme-bound copper and an exogenous electron donor. Properties of this enzyme have been recently reviewed (Skotland & Ljones, 1979a; Rosenberg & Lovenberg, 1980; Villafranca, 1981). In vivo, dopamine β-monooxygenase is compartmentalized to storage vesicles that support both an ATP-dependent accumulation of dopamine and the hydroxylation of dopamine to norepinephrine. The detection of high levels of ascorbic acid in vesicles derived from bovine adrenal glands implicates ascorbic acid as the physiological electron donor (Terland & Flatmark, 1975).

As summarized in eq 1, the overall reaction catalyzed by dopamine β-monooxygenase involves a formal transfer of two electrons and two protons from ascorbic acid to the products norepinephrine and water. We have analyzed the pH dependence of initial rate parameters and primary hydrogen isotope effects on these parameters in an effort to identify steps in the kinetic mechanism that involve proton transfer. Previous measurements of pH dependencies in the dopamine β-monooxygenase reaction were carried out at a single oxygen concentration, precluding a clear-cut determination of V_{max} and V_{max}/K_m parameters (Miras-Portugal et al., 1973; Craine et

† From the Department of Chemistry, University of California, Berkeley, California 94720. *Received November 1, 1982.* Supported by a research grant from the National Institutes of Health.

0006-2960/83/0422-3096$01.50/0 © 1983 American Chemical Society

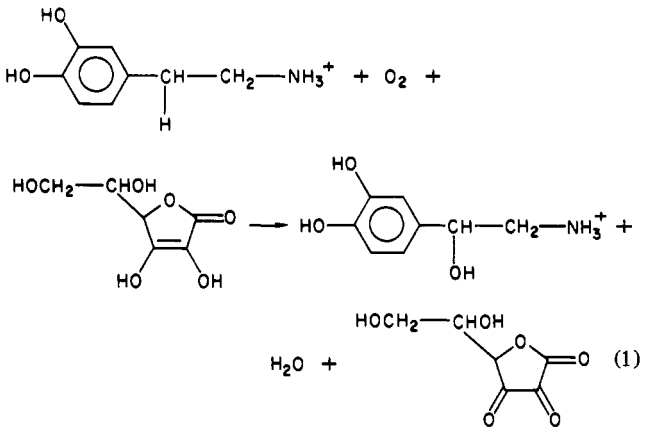

(1)

al., 1973). In the present study, dopamine β-monooxygenase activity has been monitored at varying oxygen concentrations, permitting unambiguous evaluation of V_{max}, V_{max}/K_{DM}, and V_{max}/K_{O_2}.[1]

Kinetic isotope effects measured in conjunction with pH studies provide powerful tools for the elucidation of kinetic mechanism (Cook & Cleland, 1981a,b). When intrinsic isotope effects on the isotope-sensitive steps are available [cf. Miller & Klinman (1983)], comparison of observed to intrinsic isotope effects can provide partitioning ratios and in selected instances microscopic rate constants across the experimental pH range (Miller & Klinman, 1982).

As will be shown, the available data for dopamine β-monooxygenase demonstrate an absolute requirement for a protonated form of enzyme in C–H bond cleavage, attributed to an acid-catalyzed activation of oxygen (pK = 5.6–5.8), and a preferred release of product from protonated enzyme (pK = 5.2–5.4). In addition, we observe an unprecedented dependence of kinetic order on pH such that substrate release from enzyme ternary complex is preferred ordered (oxygen off first) at pH 4.5, random at intermediate pH values, and preferred ordered (dopamine off first) at pH 6.6.

Early investigators demonstrated that certain halides and dicarboxylic acid anions activate dopamine β-monooxygenase (Levin et al., 1960; Goldstein et al., 1968; Craine et al., 1973). Fumarate, the most effective activator, has been shown to exhibit saturation kinetics, implying specific protein–anion interactions. In an effort to elucidate the molecular mechanism of anion regulation, kinetic parameters and deuterium isotope effects have been measured at varying pH values in the presence of saturating concentrations of fumarate. These studies reveal two key features regarding the activation of dopamine β-monooxygenase by fumarate: (i) a pK shift of the alkaline residue (pK = 5.6–5.8) so that enzyme remains protonated and hence optimally active over a wider pH range and (ii) a pH-dependent decrease in the rate of catecholamine dissociation, resulting in a switch in kinetic order at pH 6.6 from a preferred release of dopamine, minus fumarate, to a preferred release of oxygen, plus fumarate. The region of pH in which enzyme is most responsive to fumarate overlaps with the intravesicular pH 5.5 of bovine adrenal chromaffin vesicles, suggesting a possible regulatory mechanism for dopamine β-monooxygenase in vivo.

Experimental Procedures

Materials

All chemicals were reagent grade unless otherwise noted. Dopamine hydrochloride, norepinephrine hydrochloride, and fumaric acid were purchased from Sigma, catalase (65 000 units/mg) was from Boehringer-Mannheim, and ascorbic acid was from Aldrich. DEAE-52 ion-exchange resin and concanavalin A–Sepharose were purchased from Whatman and Pharmacia, respectively. Soluble dopamine β-monooxygenase from bovine adrenal glands was prepared as described previously (Klinman & Krueger, 1982).

Synthesis of 2-(3,4-Dihydroxyphenyl)[2-$^2H_2$]ethylamine Hydrochloride ([2-$^2H_2$]Dopamine Hydrochloride). Eighty milliliters of D_2O was added to 10 g of dry (3,4-dimethoxyphenyl)acetonitrile (0.057 mol) and 20 g of Na_2CO_3 (0.189 mol), and the mixture was stirred overnight at 50 °C. The deuterated (3,4-dimethoxyphenyl)acetonitrile product (0.031 mol) in 400 mL of ether was added dropwise over 70 min to a stirred solution of 0.033 M $LiAlH_4$ and 0.033 M $AlCl_3$ in 150 mL of ether, and the mixture was stirred for an additional hour. The reaction was quenched by addition of water (5 mL) followed by 75 mL of 3.5 N H_2SO_4 and the acidic aqueous layer extracted and adjusted to pH 11 with KOH. The resulting basic aqueous layer was extracted 3 times with ether, dried, and acidified with gaseous HCl, yielding 2-(3,4-dimethoxyphenyl)[2-$^2H_2$]ethylamine hydrochloride as a yellow oil. The dimethoxy product was converted to catechol by heating under anaerobic reflux with 48% HBr for 7 h. Solvent was evaporated under reduced pressure and the residue converted to the HCl salt by repeated dissolution in 4 N HCl and solvent removal. Further purification was carried out on Bio-Rad AG50WX12 anion-exchange resin (1.0 × 10 cm column), equilibrated in 0.1 N HCl. Dopamine hydrochloride was eluted with 4 N HCl, evaporated under reduced pressure, and recrystallized from MeOH/ether. Purity was established by thin-layer chromatography and ^1H NMR. Isotope effects using 50:50 mixtures of [2-$^2H_2$]dopamine and [2-$^1H_2$]dopamine confirmed the absence of inhibitory contaminants in the synthesized material. [2-$^1H_2$]Dopamine prepared synthetically yielded the same kinetic parameters as dopamine obtained commercially.

Methods

Absorbance spectroscopic determinations were carried out on a Cary 118 UV–vis spectrophotometer, fluorescence assays on a Perkin-Elmer Model MPF-44A fluorescence spectrophotometer, and oxygen uptake assays on a Yellow Springs Instrument Model 53 biological oxygen monitor. A Radiometer pH meter type PHM26 was used for determination of pH.

Measurement of Enzyme Activity. In the preparation of enzyme, activity was measured fluorometrically (Von Euler & Floding, 1955). For kinetic experiments, activity was measured as the rate of oxygen consumption with a polarographic oxygen electrode. In the latter assay, individual reaction mixtures were made within 15–20 min of rate measurements by mixing aliquots of concentrated stock solutions. Reaction mixtures were buffered with either 50 mM sodium phosphate or 50 mM sodium acetate, and the total ionic strength was adjusted to 0.14 M with NaCl. We have found that lowered activities and complex kinetic behavior may result unless exogenous $CuSO_4$ is added to reaction mixtures as noted originally by Skotland & Ljones (1979b); although the optimal $CuSO_4$ concentration varies with total enzyme concentration, 1.0 μM $CuSO_4$ activates the enzyme fully under conditions of these experiments, 2.5–5.0 μg/mL dopamine β-monooxygenase. All assay mixtures contained 10 mM ascorbic acid, 10 μg/mL catalase, and 1.0 μM $CuSO_4$ and were measured at 35 °C. Initial velocities were measured at varying concentrations of oxygen and dopamine. Oxygen and nitrogen (Ohio Chemical and Surgical Equipment Co.) were mixed to

[1] Abbreviations: DM, dopamine; NMR, nuclear magnetic resonance.

Table I: Steady-State Parameters and Their Deuterium Isotope Effects in Terms of Microscopic Rate Constants Described in Scheme I

Steady-State Parameters		Deuterium Isotope Effects	
$V_{max} = \frac{k_5 k_7}{k_5 + k_7}$	(1)	${}^{D}(V_{max}) = \frac{k_{5H}/k_{5D} + k_5/k_7}{1 + k_5/k_7}$	(4)
$V_{max}/K_{DM} = \frac{k_{3DM} k_5}{k_{4DM} + k_5}$	(2)	${}^{D}(V_{max}/K_{DM}) = \frac{k_{5H}/k_{5D} + k_5/k_{4DM}}{1 + k_5/k_{4DM}}$	(5)
$V_{max}/K_{O_2} = \frac{k_{3O_2} k_5}{k_{4O_2} + k_5}$	(3)	${}^{D}(V_{max}/K_{O_2}) = \frac{k_{5H}/k_{5D} + k_5/k_{4O_2}}{1 + k_5/k_{4O_2}}$	(6)

obtain the desired oxygen concentrations, which were standardized against air-saturated distilled water at 35 °C. Concentrations of dopamine were determined spectrophotometrically with an extinction coefficient of $\epsilon^{1cm}_{280nm} = 2670\ M^{-1}\ cm^{-1}$. In the determination of deuterium isotope effects, enzyme activities were measured by alternating between deuterated and protonated dopamine to minimize differences in reaction conditions at single substrate concentrations.

Calculation of Kinetic Constants. In the statistical analysis of our kinetic data, four nonlinear least-squares computer programs were used, which were written by Cleland (1979) and translated to BASIC for use on a NorthStar Horizon computer. Enzyme activities vs. substrate concentration at fixed concentrations of alternate substrate were fit to the expression

$$\frac{v}{E_T} = \frac{V_{max}(app)S}{K_m(app) + S} \quad (2)$$

using the program HYPER with weighting factors set to unity. Limiting kinetic constants were calculated by refitting $V_{max}(app)$ and $V_{max}/K_m(app)$ values vs. alternative substrate concentrations to the same expression, using weighting factors that were generated in the first cycle. In eq 2, velocities were divided by enzyme concentration, assuming a subunit M_r of 75 000; thus V_{max} and V_{max}/K_m are rate constants with units of s^{-1} and $M^{-1}\ s^{-1}$, respectively. Deuterium isotope effects were then calculated as the ratios of the limiting kinetic parameters for protonated to deuterated substrates. In analyzing pH profiles, all V_{max}/K_m parameters (plus or minus fumarate) were fit to the expression

$$\log v = \log \frac{C}{1 + [H^+]/K_A + K_B/[H^+]} \quad (3)$$

by using the program BELL, where C is pH independent. V_{max} and k_7 parameters (plus or minus fumarate) were fit to the expression

$$\log v = \log \frac{V_1 + V_2(K/[H^+])}{1 + K/[H^+]} \quad (4)$$

by using the program WAVL, and the k_{3O_2} parameters (plus or minus fumarate) were fit to the expression

$$\log k = \log \frac{C}{1 + K/[H^+]} \quad (5)$$

by using the program HBBELL, with C pH independent. In all pH analyses, weighting factors were equal to unity.

Results

Definition of V_{max}, V_{max}/K_{O_2}, and V_{max}/K_{DM} and ${}^{D}(V_{max})$, ${}^{D}(V_{max}/K_{O_2})$, and ${}^{D}(V_{max}/K_{DM})$ for a Minimal Kinetic Mechanism. Previous work has shown that the tritium isotope effect for the dopamine β-monooxygenase catalyzed hydroxylation of [^{3}H]dopamine in the absence of fumarate, pH 6.0, is greater than unity in the limit of infinite oxygen, proving that substrates dopamine and oxygen can undergo random addition to enzyme to form a ternary enzyme complex prior to hydrogen abstraction (Klinman et al., 1980). In addition, the absence of back-incorporation of tritium from solvent into dopamine under turnover conditions implies irreversibility of C–H bond cleavage (Miller & Klinman, 1983). On the basis of these results, a minimal kinetic scheme for substrate binding and catalysis is written in Scheme I, where product release is assumed irreversible under conditions of initial rates.

Scheme I: Minimal Kinetic Mechanism for Random Addition of Dopamine and Oxygen to Dopamine β-Monooxygenase Followed by Irreversible Catalytic and Product Release Steps

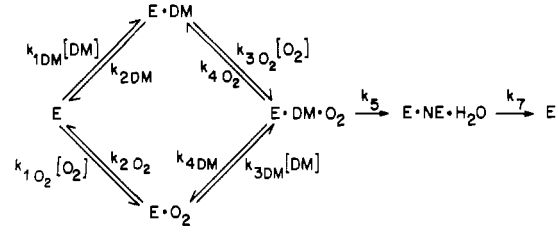

Although it is well established that enzyme-bound copper(II) undergoes a one-electron reduction to copper(I) concomitant with the one-electron oxidation of ascorbate to semidehydroascorbate (Skotland & Ljones, 1980; Diliberto & Allen, 1981), a subsequent step for the binding of ascorbate to either binary or ternary complexes may occur. In order to minimize ambiguities arising from the position of reductant binding/oxidation, ascorbate was maintained at high saturating levels (10 mM) throughout these studies.

Three limiting kinetic parameters are obtained from initial velocity studies: V_{max}/K_{O_2} and V_{max}/K_{DM}, extrapolated to infinite dopamine or oxygen concentrations, respectively, and V_{max}, extrapolated to infinite levels of both substrates. In Table I, eq 1–3, these parameters are expressed in terms of the microscopic rate constants defined in Scheme I. It can be seen that V_{max}/K_{O_2} and V_{max}/K_{DM} reflect net rate constants for the addition of oxygen and dopamine to the binary complexes E·DM and E·O_2, together with the subsequent activation of the substrate ternary complex. V_{max} represents the net rate constant for the regeneration of free enzyme from the substrate ternary complex, which includes both the chemical conversion and product release steps.

Expressions for the deuterium isotope effects, ${}^{D}(V_{max})$, ${}^{D}(V_{max}/K_{O_2})$, and ${}^{D}(V_{max}/K_{DM})$ are also given in Table I, eq 4–6. In the derivation of these expressions, k_5 is attributed to the C–H bond cleavage step and assumed to be the sole isotope-dependent step. Recently, the intrinsic isotope effect on k_5 has been measured as 9.4 ± 1.3 in the presence of 10 mM fumarate and 10.9 ± 1.9 in the absence of fumarate (Miller & Klinman, 1983). According to eq 4–6 of Table I,

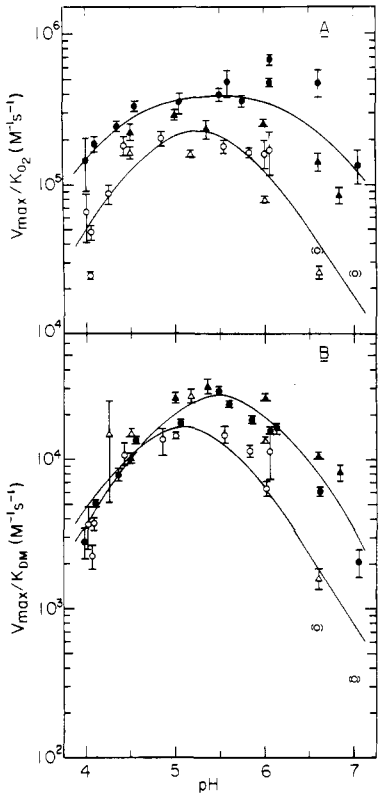

FIGURE 1: pH dependences of V_{max}/K_{O_2} (A) and V_{max}/K_{DM} (B) in the presence (●) and absence (○) of 10 mM fumarate. The assay mixtures in these and all other experiments contained 10 mM ascorbate, 650 units/mL catalase, and 1 μM $CuSO_4$ and were buffered with 50 mM sodium phosphate or sodium acetate. Total ionic strength was adjusted with NaCl to 0.14 M. Circles and triangles show the variation in kinetic values using two different enzyme preparations. Theoretical curves were calculated by using the program BELL by Cleland (1979).

the magnitude of observed isotope effects on V_{max}, V_{max}/K_{O_2}, and V_{max}/K_{DM} will be diminished from the intrinsic isotope effect by the partitioning ratios of k_5/k_7, k_5/k_{4O_2}, and k_5/k_{4DM}, respectively.

The mechanistic significance of rate constants in eq 1–6 of Table I depends upon assumptions underlying the development of a minimal kinetic mechanism. Specifically, interpretation of k_5 and k_7 depends on the kinetic significance of chemical steps subsequent to the first irreversible C–H bond cleavage step. If the chemical conversion of dopamine to norepinephrine occurs either in a single step or in several fast steps following a slow C–H bond activation step, k_5 and k_7 remain as defined in Scheme I. Alternatively, if slow chemical step(s) followed C–H cleavage, it would be necessary to redefine these rate constants with k_5 representing the first irreversible C–H bond cleavage step to generate a new ternary enzyme complex, E′, and k_7 representing both chemical and dissociation steps for the regeneration of free enzyme from E′. In the dopamine β-monooxygenase reaction, where the magnitude of the intrinsic isotope effect approaches the theoretical limit and product release is rate limiting, it is unlikely that C–H bond cleavage can be irreversible unless this step is stepwise and rate limiting relative to any subsequent chemical steps [cf. Miller & Klinman (1983)]; we therefore believe the former model is the correct representation of the dopamine β-monooxygenase mechanism.

pH Dependence of V_{max}, V_{max}/K_{O_2}, and V_{max}/K_{DM}, Plus or Minus Fumarate. The pH dependences for V_{max}, V_{max}/K_{O_2}, and V_{max}/K_{DM} in the absence of fumarate are presented in Figures 1 and 2, open circles. V_{max}/K_m vs. pH plots, illustrated

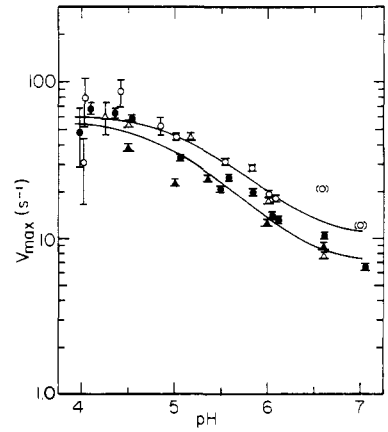

FIGURE 2: pH dependence of V_{max} in the presence (●) and absence (○) of 10 mM fumarate. Circles and triangles represent two different enzyme preparations. Theoretical curves were calculated by using the program WAVL by Cleland (1979).

Table II: Apparent pK Values and Limiting Rate Constants Derived from Least-Squares Analyses of Figures 1 and 2

parameter		−fumarate	+fumarate
V_{max}/K_{O_2}	pK_A[a]	4.86 ± 0.13	4.32 ± 0.10
	pK_B	5.63 ± 0.13	6.60 ± 0.10
	C	(4.16 ± 0.92) × 10^5 M^{-1} s^{-1}	(4.53 ± 0.38) × 10^5 M^{-1} s^{-1}
V_{max}/K_{DM}	pK_A[a]	4.78 ± 0.04[c]	5.06 ± 0.07
	pK_B	5.38 ± 0.04[c]	5.90 ± 0.07
	C	(3.28 ± 0.19) × 10^4 M^{-1} s^{-1}	(4.71 ± 0.51) × 10^4 M^{-1} s^{-1}
V_{max}	pK[b]	5.39 ± 0.25	5.19 ± 0.14
	V_1	62.1 ± 1.7	56.8 ± 1.2
	V_2	9.84 ± 1.25 s^{-1}	6.66 ± 0.44 s^{-1}

[a] pK_A, pK_B, and C are defined in eq 3 under Methods. [b] pK, V_1, and V_2 are defined in eq 4 under Methods. [c] Data were fit by assuming a pK separation of 0.6.

in Figure 1, are bell shaped with slopes of ca. −1 and 1 on either side of maxima corresponding to $V_{max}/K_{O_2} = 4.2 \times 10^5$ M^{-1} s^{-1} and $V_{max}/K_{DM} = 3.3 \times 10^4$ M^{-1} s^{-1} (Table II). While recent literature emphasizes that the interpretation of slopes in pH plots will vary with the complexity of the kinetic mechanism (Cleland, 1977; Knowles, 1976), evidence is presented below showing that some of the pK values appearing in the V_{max}/K_m plots represent microscopic pKs. The apparent pK_A = 4.8–4.9 and pK_B = 5.4–5.6 in the absence of fumarate are smaller than the ionization constants for dopamine and are almost identical for both V_{max}/K_m parameters, implicating the ionization of enzyme-bound residues that appear insensitive to the form of enzyme binary complex, i.e., E·O_2 in the case of V_{max}/K_{DM} vs. E·DM in the case of V_{max}/K_{O_2}. In contrast to V_{max}/K_m, V_{max} is only moderately affected by pH. As illustrated in Figure 2, open circles, activity decreases 6-fold from 62 to 9.8 s^{-1} in the pH range 4.0–7.0. The log V_{max} vs. pH plot shows a single pK ≈ 5.4 and a slope of ca. −0.5, consistent with finite (nonzero) values for V_{max} at extremes of the experimental pH range.

The modulation of kinetic parameters by fumarate anion was also examined in the pH range 4.0–7.0, Figures 1 and 2, closed circles. Data were collected in the presence of 10 mM fumarate, which is a saturating concentration throughout the pH range; an apparent activator constant of 2 mM was observed at pH 6.0, in agreement with the value reported by May et al. (1981) using tyramine as substrate. In the presence of fumarate, V_{max}/K_{O_2} and V_{max}/K_{DM} again appear as bell-shaped

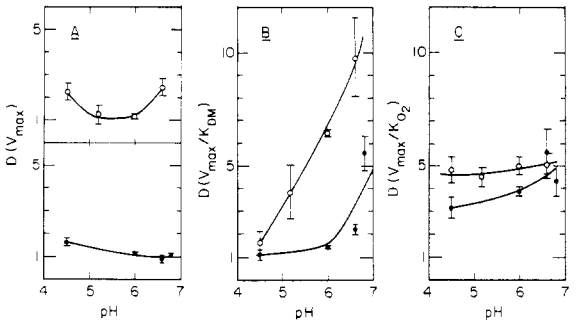

FIGURE 3: pH dependence of $^{D}(V_{max})$ (A), $^{D}(V_{max}/K_{DM})$ (B), and $^{D}(V_{max}/K_{O_2})$ (C) measured using [2-^{2}H]dopamine. Isotope effects were obtained in the presence (●) and absence (○) of 10 mM fumarate, by using a single enzyme preparation, represented by the triangles in Figures 1 and 2.

curves, and V_{max} decreases with increased pH. Activation of V_{max}/K_{DM} and V_{max}/K_{O_2} by fumarate is primarily expressed by basic shifts in the pK = 5.4–5.6 range, so that the plateau regions of maximal activity extend to higher values. As shown in Figure 1, fumarate increases V_{max}/K_m 5–10-fold in the pH range 5.0–6.5, indicating that the pH region with maximal sensitivity to fumarate in vitro overlaps with the intravesicular pH ≃5.5 reported for bovine adrenal chromaffin vesicles (Njus & Radda, 1978). In marked contrast to V_{max}/K_m, fumarate decreases the magnitude of V_{max} by 10–30% across the experimental pH range with no apparent shift in pK.

pH Dependence of $^{D}(V_{max})$, $^{D}(V_{max}/K_{O_2})$, *and* $^{D}(V_{max}/K_{DM})$, *Plus or Minus Fumarate.* Deuterium isotope effects were measured with [2-^{2}H$_2$]dopamine as substrate, due to the ease of synthesis of this substrate on the requisite gram scale. Although measured isotope effects will therefore reflect the product of primary and secondary effects, the small magnitude of the secondary effect is expected to make a negligible contribution to observed values.

Isotope effect data are plotted as functions of pH, Figure 3. In the absence of fumarate, $^{D}(V_{max})$ is nearly 1.0 in the pH region 5.0–6.0, increasing to 2.3 at pH 4.5 and to 2.6 at pH 6.6 (Figure 3A, open circles). These data indicate that at high and low pH values the chemical conversion step, k_5, is partially rate limiting. However, since at all pH values the magnitude of the observed isotope effect on V_{max} is small relative to k_{5H}/k_{5D} = 9.4–10.9, we conclude that V_{max} is mainly controlled by product dissociation. The addition of fumarate leads to $^{D}(V_{max})$ values close to 1.0 at all pHs and, hence, full rate limitation by product release over a wider pH range. Clearly, the magnitude of V_{max} primarily reflects a single step, k_7, under all experimental conditions; from the pH dependence of V_{max}, we estimate a pK = 5.2–5.4 for the ionization of E·NE·H_2O, which appears insensitive to the presence of fumarate. From the observed reduction in V_{max} and $^{D}(V_{max})$, reflecting a decrease in k_7 and an increase in k_5/k_7, respectively, we ascribe the primary effect of fumarate on V_{max} to a reduction in the rate constant for product release.

Isotope effects on V_{max}/K_{O_2}, Figure 3C, vary slightly with pH and fumarate, indicating very modest changes in k_5/k_{4O_2}. According to eq 3 in Table I, the pH dependence of V_{max}/K_{O_2} reflects the behavior of k_{3O_2} when k_5/k_{4O_2} is invariant; hence, the decreases in V_{max}/K_{O_2} below pH 4.5 and above pH 6.5 can be attributed directly to k_{3O_2}. The same reasoning applies in the presence of fumarate, where k_5/k_{4O_2} is again nearly independent of pH, although the slight decrease in $^{D}(V_{max}/K_{O_2})$ indicates a small increase in the magnitude of k_5/k_{4O_2}. Thus, we conclude that apparent pK values that appear in V_{max}/K_{O_2} plots (plus or minus fumarate) reflect microscopic pK values

Scheme II: pH Dependence of Minimal Kinetic Mechanism in Scheme I Assuming Ionization of Two Enzyme Residues, B1 and B2[a]

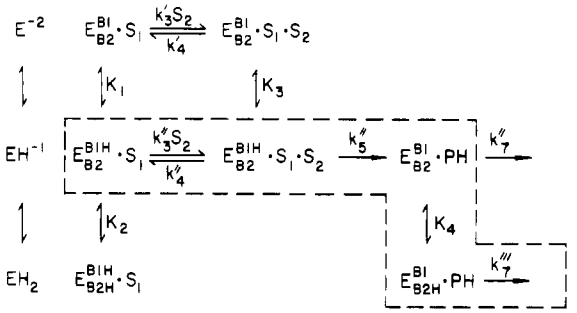

[a] S_1 and S_2, respectively, represent first and second substrates bound. Broken lines indicate the preferred route of enzyme turnover.

controlling the binding of oxygen to E·DM and that the presence of fumarate decreases the ionization constant for the basic residue (pK = 5.6) by about 10-fold.

In contrast to $^{D}(V_{max}/K_{O_2})$, $^{D}(V_{max}/K_{DM})$ increases markedly above pH 4.5, approaching the intrinsic isotope effect of 10.9 at pH 6.6 (Figure 3B, open circles). *Therefore,* V_{max}/K_{DM} *at high pH is the only measurement under which the isotopically sensitive step,* k_5, *is almost completely rate limiting, and exploration of the mechanistic nature of* k_5 *must take this into account.* Whereas the increase in $^{D}(V_{max}/K_{DM})$ can be attributed to a decrease in the partitioning ratio k_5/k_{4DM}, the fall-off in V_{max}/K_{DM} below pH 4.5, where $^{D}(V_{max}/K_{DM})$ is close to 1.0, must arise in large part from a decrease in the rate of dopamine binding to E·O_2 (i.e., k_{3DM}). The addition of fumarate leads to a marked reduction in $^{D}(V_{max}/K_{DM})$ to values equal to or slightly greater than 1.0 at pH values below pH 6.0, indicating rate limitation of V_{max}/K_{DM} by k_{3DM} in this pH range. The large increase in k_5/k_{4DM} upon addition of fumarate contrasts with a modest effect on k_5/k_{4O_2}, suggesting that a major role for fumarate in V_{max}/K_{DM} activation is the reduction in the rate of dopamine dissociation from enzyme–substrate ternary complex.

Discussion

Expansion of Minimal Kinetic Mechanism To Include pH-Dependent Steps. The bell-shaped V_{max}/K_m curves in Figure 1 signify the presence of at least three ionization states for dopamine β-monooxygenase, which may represent binary or ternary enzyme–substrate and enzyme–product complexes. In Scheme II we have expanded the mechanism in Scheme I, invoking the ionization of two residues, B1 and B2, which are the minimal number of residues required to account for this pH dependence. The existence of the binary complexes E^{B1}_{B2}·S, E^{B1H}_{B2}·S, and E^{B1H}_{B2H}·S follows from the pH behavior of k_{3O_2} across the pH range and k_{3DM} below pH 6.0. In addition, the finite limiting values of V_{max} at high and low pH require that two ionization states of the ternary enzyme–product complex be catalytically viable. Because V_{max} is almost completely limited by the product release step, k_7, we attribute the pK = 5.2–5.4 in V_{max} vs. pH (Figure 2) to pK_4 and infer that a third enzyme–product ternary complex is absent. Although initial rate parameters provide no direct evidence for the existence of the ternary enzyme–substrate complexes E^{B1}_{B2}·S_1·S_2 and E^{B1H}_{B2H}·S_1·S_2, data implicating the presence of E^{B1}_{B2}·S_1·S_2 as well as the absence of an alkaline enzyme product complex will be presented below.

In Scheme II, each rate constant is modulated by no more than two pKs. Since K_3 represents the ionization of the ter-

Table III: pH Dependences of Initial Rate Parameters, Deuterium Isotope Effects, and Rate Constants Derived According to Scheme II

$$V_{max} = \frac{k''_5\left(k''_7 + k'''_7\frac{[H^+]}{K_4}\right)}{\left(\frac{K_3}{[H^+]} + 1\right)\left(k''_7 + k'''_7\frac{[H^+]}{K_4}\right) + k''_5\left(1 + \frac{[H^+]}{K_4}\right)} \quad (1)$$

$$V_{max}/K_m = \frac{k''_5\left(k'_3\frac{K_1}{[H^+]} + k''_3\right)}{\left(\frac{K_1}{[H^+]} + 1 + \frac{[H^+]}{K_2}\right)\left(k''_5 + k''_4 + k'_4\frac{K_3}{[H^+]}\right)} \quad (2)$$

$$^D(V_{max}) = \frac{k_5H/k_5D + C^a}{1 + C} \quad (3)$$

$$^D(V_{max}/K_m) = \frac{k_5H/k_5D + C^b}{1 + C} \quad (4)$$

$$k_3 = \frac{k'_3\frac{K_1}{[H^+]} + k''_3}{\frac{K_1}{[H^+]} + 1 + \frac{[H^+]}{K_2}} \quad (5)$$

$$k_4 = \frac{k'_4\frac{K_3}{[H^+]} + k''_4}{\frac{K_3}{[H^+]} + 1} \quad (6)$$

$$k_5 = \frac{k''_5}{\frac{K_3}{[H^+]} + 1} \quad (7)$$

$$k_7 = \frac{k''_7 + k'''_7\frac{[H^+]}{K_4}}{1 + \frac{[H^+]}{K_4}} \quad (8)$$

[a] $C = k''_5(1 + [H^+]/K_4)/[(K_3/[H^+] + 1)(k''_7 + k'''_7[H^+]/K_4)]$. [b] $C = k''_5/(k'_4K_3/[H^+] + k''_4)$.

nary–substrate complex, it is reflected in the rate constants k_4 and k_5. Similarly, k_3 reflects ionizations of the enzyme binary complexes represented by K_1 and K_2, which may differ depending on the identity of the bound substrate, and k_7 reflects the ionization of the enzyme–product complex, K_4. For a model in which proton ionizations are in rapid equilibrium, the steady-state derivation of the pH dependences for kinetic parameters, isotope effects, and microscopic rate constants leads to eq 1–8, Table III. As discussed by Fersht (1977), points of inflection in pH profiles are determined by terms in the denominator. Consequently, apparent pKs for rate constants vs. pH yield microscopic pKs, while in general, apparent pKs for kinetic parameters and isotope effects are displaced from microscopic pKs by selected ratios of rate constants.

As discussed under Results, the pH dependence of $^D(V_{max}/K_{O_2})$ and $^D(V_{max}/K_{DM})$ indicates that the $pK_A = 4.9$ (minus fumarate) and $pK_A = 4.3$ (plus fumarate) observed in V_{max}/K_{O_2} vs. pH plots and the $pK_A = 5.1$ in the V_{max}/K_{DM} vs. pH plot (plus fumarate) reflect microscopic pK values for the ionization of B2 (pK_2 in Table IV), with both oxygen and dopamine undergoing preferential binding to unprotonated enzyme, $E_{B2}^{B1H}\cdot S_1$. It is significant that the pK_2 derived from V_{max}/K_m plots is similar to the pK = 5.2–5.4 in V_{max} and that both ionizations appear insensitive to the presence of anion activator. These observations support the assignment of pK_4 to the ionization of B2.

The plots of V_{max}/K_m vs. pH (Figure 1) clearly implicate

Table IV: Microscopic pK_a Values in the Dopamine β-Monooxygenase Reaction[a]

constant[a]	value −fumarate	value +fumarate	rationale
pK_1(E·DM)	5.62 ± 0.13	6.60 ± 0.09	log (V_{max}/K_{O_2}) (Figure 1)
	5.85 ± 0.02	6.81 ± 0.18	log $k_{3\,O_2}$ vs. pH (Figure 4)
pK_1(E·O_2)	i	i	
pK_2(E·DM)	4.86 ± 0.13	4.32 ± 0.10	log (V_{max}/K_{O_2}) vs. pH (Figure 1)
pK_2(E·O_2)	4.78 ± 0.03	5.06 ± 0.07	log (V_{max}/K_{DM}) vs. pH (Figure 1)
pK_3	i	i	
pK_4	5.39 ± 0.25	5.19 ± 0.14	log V_{max} vs. pH (Figure 2)
	5.41 ± 0.03	5.40 ± 0.21	log k_7 vs. pH[b]

[a] These constants refer to the ionization in Scheme II. Indeterminate values indicated as i. [b] Data not shown.

a second residue, B1, in catalysis. As we have noted, the magnitude of $^D(V_{max}/K_{DM})$ approaches $k_{5\,H}/k_{5\,D}$ at high pH in the absence of fumarate, meaning that the partitioning ratio, $k_5/k_{4\,DM}$ (eq 4 in Table III), approaches zero when $[H^+] \ll K_3$. As Cook & Cleland (1981a) have shown, this result is diagnostic of loss of a proton from $E_{B2}^{B1H}\cdot S_1\cdot S_2$ to generate $E_{B2}^{B1}\cdot S_1\cdot S_2$, which cannot proceed to product, $k'_5 = 0$, but which is competent to regenerate free enzyme; i.e., $k'_{3\,DM}$ and $k'_{4\,DM}$ are finite. While these data imply that B1 must be protonated for interconversion of ternary complex, deuterium isotope effects in the pH range 5.0–7.0 indicate a complex kinetic expression for V_{max}/K_{DM} with no single rate constant dominating; hence, the $pK_B = 5.4$ (Table II) does not permit quantitation of K_3. Saturating concentrations of fumarate both decrease $^D(V_{max}/K_{DM})$ and shift the pK_B to 5.9. To the extent that addition of fumarate alters the rate constants controlling the V_{max}/K_{DM} expression, i.e., below pH 6.6 $^D(V_{max}/K_{DM}) \leq 2.2$ indicating domination of V_{max}/K_{DM} by $k_{3\,DM}$, the magnitude of pK_B is expected to increase (cf. the discussion of the pH dependences of $k_{3\,DM}$ and k_5 under microscopic constants). Therefore, the basic shift observed on V_{max}/K_{DM} above pH 5.0 upon adding fumarate can be attributed to changes in the rate-determining step, together with possible perturbations of K_1 for the ionization of $E_{B2}^{B1H}\cdot O_2$. Evidence in support of a perturbation in the ionization of $E_{B2}^{B1H}\cdot DM$ by fumarate was deduced from the behavior of V_{max}/K_{O_2} above pH 5.8. Calculated values for $k_{3\,O_2}$ vs. pH will be presented below, which allow direct estimation of pK_1 (E·DM), plus or minus fumarate.

While the kinetic expressions for the pH dependences of V_{max} and $^D(V_{max})$ contain both K_3 and K_4 (eq 1 and 3 in Table III), the V_{max} vs. pH plots show a single low pK = 5.2–5.4 that we have assigned to K_4. This is a result of the dominance of k_5 by k_7 in the experimental pH range. At pH 7.0, however, we expect k_5 to begin to become rate limiting as it approaches zero, leading to a decrease in V_{max} with an apparent pK arising but displaced from K_3. Concomitant with such a decrease in V_{max}, $^D(V_{max})$ is expected to approach $k_{5\,H}/k_{5\,D}$ as the partitioning ratio k_5/k_7 diminishes. Whereas the anticipated increase in $^D(V_{max})$ appears at pH 6.6 in the absence of fumarate, $^D(V_{max})$ remains close to 1.0 in the presence of fumarate. This result is consistent with a modest effect of fumarate on k_7, together with a marked reduction in K_3, analogous to the perturbation of K_1.

Partitioning Ratios Indicate Degree of Randomness in Kinetic Mechanism. As described earlier, the magnitude of $^D(V_{max}/K_{DM})$ in the limit of infinite oxygen concentration measures the randomness in the dopamine β-monooxygenase kinetic mechanism. When $^D(V_{max}/K_{DM}) = 1.0$ and $^D(V_{max}/$

Table V: Partitioning Ratios $k_5/k_{4\,DM}$, $k_5/k_{4\,O_2}$, and $k_{4\,O_2}/k_{4\,DM}$ as Functions of pH and Fumarate

pH	condition	$k_5/k_{4\,DM}$	$k_5/k_{4\,O_2}$	$k_{4\,O_2}/k_{4\,DM}$
4.5	−fumarate	14.9	1.62	9.2
5.2	−fumarate	2.48	1.83	1.4
6.0	−fumarate	0.835	1.50	0.56
6.6	−fumarate	0.140	1.49	0.094
6.6	+fumarate	5.89	0.832	7.1

K_{O_2}) is finite, the kinetic mechanism is ordered with oxygen release from enzyme ternary complex preceding dopamine (Klinman et al., 1980). The data in Figure 3B indicate that in the pH range 4.5–6.0 fumarate converts a random kinetic mechanism to an ordered one. Above pH 6.0, the nonunity value for $^{D}(V_{max}/K_{DM})$ indicates a random component even in the presence of fumarate.

Kinetic order can be estimated more quantitatively from the magnitudes of $^{D}(V_{max}/K_{DM})$ and $^{D}(V_{max}/K_{O_2})$. If one employs values for the intrinsic isotope effect of $k_{5\,H}/k_{5\,D}$ = 10.9 ± 1.9, minus fumarate, and 9.4 ± 1.3, plus fumarate, eq 5 and 6 in Table I directly provide the partitioning ratios $k_5/k_{4\,O_2}$ and $k_5/k_{4\,DM}$, from which $k_{4\,O_2}/k_{4\,DM}$ can be calculated. It should be noted that propagation of error precludes precise quantitation of partitioning ratios under conditions where experimental isotope effects approach either unity or the intrinsic isotope effect. As seen in Figure 3B, values for $^{D}(V_{max}/K_{DM})$ in the presence of fumarate are too close to unity to permit calculation of $k_5/k_{4\,DM}$ in the pH range 4.5–6.0. However, $k_5/k_{4\,DM}$ and $k_5/k_{4\,O_2}$ are available in the absence of fumarate at pH 4.5–6.6 and in the presence of fumarate at pH 6.6 (Table V). As expected, the partitioning ratios indicate an inverse behavior to their corresponding isotope effect, with $k_5/k_{4\,O_2}$ essentially constant and $k_5/k_{4\,DM}$ decreasing dramatically from pH 4.5 to 6.6.

The tabulated values for $k_{4\,O_2}/k_{4\,DM}$, minus fumarate, show an unexpected trend as a function of pH. At pH 4.5, the kinetic mechanism is ordered with oxygen dissociating 9.2-fold faster than dopamine from ternary complex. At pH 5.2 and 6.0, the kinetic mechanism is completely random, having approximately equal rates for oxygen and dopamine dissociation. Above pH 6.0, the kinetic mechanism is once again ordered, but with preferential release of dopamine. The data at pH 6.0 can be compared to a previous study that measured $^{T}(V_{max}/K_{DM})$ in the absence of exogenous $CuCl_2$; under these conditions, $k_{4\,O_2}/k_{4\,DM}$ was found to be 6 (Klinman et al., 1980). While the 11-fold difference in $k_{4\,O_2}/k_{4\,DM}$ as a function of added Cu(II) indicates a role for this effector on the rate of dopamine/oxygen release from ternary complex, careful studies are required to elucidate the precise mechanism of exogenous copper activation.

The mechanistic origin of the changeover in kinetic order is best understood from the pH dependences of $k_5/k_{4\,DM}$ and $k_5/k_{4\,O_2}$. The partitioning ratio of $k_5/k_{4\,O_2}$ is essentially invariant in the pH range 4.5–6.6, implying identical pH dependences for k_5 and $k_{4\,O_2}$. From eq 7 in Table III, it is shown that $k_5 = k''_5/(K_3/[H^+] + 1)$. In order to obtain an identical pH dependence for $k_{4\,O_2}$, the term $K_3/[H^+]$ must be contained solely in the denominator of $k_{4\,O_2}$ (eq 6 in Table III), meaning that $k'_{4\,O_2}(K_3/[H^+])$ is insignificant relative to k''_{4O_2} in the experimental pH range. The mechanistic consequence is a highly preferred release of oxygen from $E^{B1H}_{B2}\cdot S_1\cdot S_2$ than from $E^{B1}_{B2}\cdot S_1\cdot S_2$, Scheme II. In contrast to $k_5/k_{4\,O_2}$, $k_5/k_{4\,DM}$ decreases 100-fold in the pH range 4.5–6.6. This behavior is consistent with opposing trends in $k_{4\,DM}$ and k_5, so that the decrease in $k_5/k_{4\,DM}$ can be attributed to an increase in $k_{4\,DM}$ to a limiting value of $k'_{4\,DM}$ supplemented by a fall-off in k_5 at pH values above K_3. Thus, in addition to confirming the conclusion that dopamine undergoes dissociation from $E^{B1}_{B2}\cdot S_1\cdot S_2$, the pH dependence of $k_5/k_{4\,DM}$ suggests that $k'_{4\,DM} > k''_{4\,DM}$. This point is considered in greater detail below. Importantly, it is the ability of dopamine to dissociate from $E^{B1}_{B2}\cdot S_1\cdot S_2$ coupled with the highly preferred release of oxygen from $E^{B1H}_{B2}\cdot S_1\cdot S_2$ that leads to the observed switch in kinetic mechanism from a preferential release of oxygen at pH 4.5 to a preferential release of dopamine at pH 6.6 (Table V).

As noted earlier, initial rate data do not provide information regarding the kinetic significance of a third enzyme–substrate ternary complex, $E^{B1H}_{B2H}\cdot S_1\cdot S_2$. Simulations of eq 6 in Table III (assuming that $pK_3 = pK_1$) show that the large 100-fold increase in $k_{4\,O_2}/k_{4\,DM}$ from pH 6.6 to 4.5 can be fully accounted for by a decrease in $k_{4\,DM}$ and an increase in $k_{4\,O_2}$ below pK_3. Therefore, $E^{B1H}_{B2H}\cdot S_1\cdot S_2$ is omitted from Scheme II, in the absence of more complete data. In support of this scheme, V_{max}/K_{O_2} (minus fumarate) decreases below pH 4.5 with a slope $\simeq$ 1.0, implying that, at least in the absence of fumarate, $k'''_{3\,O_2} = 0$.

The presence of fumarate also has a marked effect on $k_{4\,O_2}/k_{4\,DM}$, which at pH 6.6 increases from 0.094, minus fumarate, to 7.1, plus fumarate. This result implicates a role for fumarate in the conversion of dopamine β-monooxygenase from an "alkaline" to an "acidic" form. As discussed below, this conversion is a consequence of significant decreases in both $k_{4\,DM}$ and K_3 in the presence of anion effector.

Calculation of Microscopic Constants. Equations 1–6 in Table I show six equations in seven unknowns, $k_{3\,O_2}$, $k_{3\,DM}$, $k_{4\,O_2}$, $k_{4\,DM}$, k_5, k_7, and $k_{5\,H}/k_{5\,D}$. Independent determination of $k_{5\,H}/k_{5\,D}$ allows, in principle, explicit solutions for all rate constants. By combining and rearranging eq 1–6, expressions have been derived for each microscopic rate constant in terms of the experimentally measured parameters (steady-state parameters, observed isotope effects, and $k_{5\,H}/k_{5\,D}$), eq 1–4 in Table VI. Key considerations for the precise estimation of each constant are experimental error and the magnitude of observed isotope effects in relation to either unity or the intrinsic isotope effect. As described previously (Miller & Klinman, 1982), error functions can be derived from eq 1–4 of Table VI, using standard methods of error propagation, leading to eq 5–8, Table VI. These equations call attention to the major causes of the uncertainty in the rate constants; i.e., a small difference between an isotope effect and 1.0 or $k_{5\,H}/k_{5\,D}$ can contribute as greatly as a large experimental error in a measured parameter.

In the expressions for σ_{k_3} and σ_{k_7}, the terms $(^{D}k - {}^{D}V/K)$ and $(^{D}k - {}^{D}V)$ appear in the denominator, eq 5 and 8, Table VI. With the exception of pH 6.6, minus fumarate, observed isotope effects are significantly different from $k_{5\,H}/k_{5\,D}$, and the rate constants $k_{3\,O_2}$ $k_{3\,DM}$ and k_7 are well determined. In contrast, expressions for σ_{k_4} and σ_{k_5} contain the term $(^{D}V - 1)$ in their denominators. As evident from Figure 3, $^{D}(V_{max})$ is close to 1.0 over most of the experimental pH range, so that k_4 and k_5 are less well determined and in some instances indeterminate. Despite these limitations, a number of rate constants are available in the pH range 4.5–6.8 (Table VII). Unfortunately, it has not been possible to obtain microscopic constants below pH 4.5 and above pH 6.8, since K_m values for both oxygen and dopamine increase greatly, yielding unacceptable experimental error in measured isotope effects.

The constants $k_{3\,O_2}$ and k_7 are best evaluated in this study. The k_7 vs. pH plot (data not shown) is similar to the V_{max} vs. pH plot in Figure 2, a consequence of the dominance of V_{max}

Table VI: Microscopic Rate Constants and Error Functions for These Constants, in Terms of Steady-State Parameters, Isotope Effects on These Parameters, and the Intrinsic Isotope Effect[a]

constant		error function	
$k_3 \equiv \frac{(V/K)(^{D}k-1)}{[^{D}k-(^{D}V/K)]}$	(1)	$\frac{\sigma_{k_3}}{k_3} = \left[\left(\frac{\sigma_{^{D}k}[(^{D}V/K)-1]}{(^{D}k-1)[^{D}k-(^{D}V/K)]}\right)^2 + \left(\frac{\sigma_{V/K_H^{D}k}}{(V/K_H)[^{D}k-(^{D}V/K)]}\right)^2 + \left(\frac{\sigma_{V/K_D(^{D}V/K)}}{(V/K_D)[^{D}k-(^{D}V/K)]}\right)^2\right]^{1/2}$	(5)
$k_4 \equiv \frac{V[(^{D}V/K)-1](^{D}k-1)}{(^{D}V-1)[^{D}k-(^{D}V/K)]}$	(2)	$\frac{\sigma_{k_4}}{k_4} = \left[\left(\frac{\sigma_{^{D}k}[(^{D}V/K)-1]}{(^{D}k-1)[^{D}k-(^{D}V/K)]}\right)^2 + \left(\frac{\sigma_{^{D}V/K}(^{D}k-1)}{[^{D}k-(^{D}V/K)][(^{D}V/K)-1]}\right)^2 + \left(\frac{\sigma_{V_H}}{V_H(^{D}V-1)}\right)^2 + \left(\frac{\sigma_{V_D^{D}V}}{V_D(^{D}V-1)}\right)^2\right]^{1/2}$	(6)
$k_5 \equiv \frac{V(^{D}k-1)}{^{D}V-1}$	(3)	$\frac{\sigma_{k_5}}{k_5} = \left[\left(\frac{\sigma_{^{D}k}}{(^{D}k-1)}\right)^2 + \left(\frac{\sigma_{V_H}}{V_H(^{D}V-1)}\right)^2 + \left(\frac{\sigma_{V_D^{D}V}}{V_D(^{D}V-1)}\right)^2\right]^{1/2}$	(7)
$k_7 \equiv \frac{V(^{D}k-1)}{^{D}k-^{D}V}$	(4)	$\frac{\sigma_{k_7}}{k_7} = \left[\left(\frac{\sigma_{^{D}k}(^{D}V-1)}{(^{D}k-1)(^{D}k-^{D}V)}\right)^2 + \left(\frac{\sigma_{V_H^{D}k}}{V_H(^{D}k-^{D}V)}\right)^2 + \left(\frac{\sigma_{V_D^{D}V}}{V_D(^{D}k-^{D}V)}\right)^2\right]^{1/2}$	(8)

[a] The intrinsic isotope effect, k_{5H}/k_{5D}, is written as ^{D}k. $V_H/V/K_H$, V_D, and V/K_D represent V_{max} and V_{max}/K_m for protonated and deuterated substrates, respectively. $^{D}(V_{max})$ and $^{D}(V_{max}/K_m)$ are indicated as ^{D}V and $^{D}V/K$.

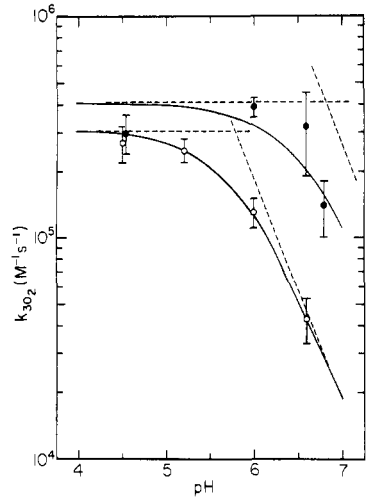

FIGURE 4: pH dependence of rate constant k_{3O_2} in the presence (●) and absence (○) of 10 mM fumarate. Theoretical curves were calculated by using the program HBBELL by Cleland (1979).

by k_7. In Figure 4, a plot of k_{3O_2} vs. pH identifies $pK_1 = 5.8$ for the binding of oxygen to E·DM, as well as a marked alkaline shift to $pK_1 \simeq 6.8$ upon addition of fumarate, confirming a direct perturbation of K_1 by anion effector. A second pK_2 below pH 4.8 is expected for the decrease in k_{3O_2}, as seen in the V_{max}/K_{O_2} profile; however, the data do not extend to a low enough pH to verify this prediction. The data for k_{3DM} may be accounted for by either an insensitivity to pH for dopamine binding to the enzyme–oxygen complex or a greater pK perturbation so that a significant change in k_{3DM} is not apparent at pH 6.8, plus or minus fumarate.

Although data for k_{4O_2} and k_5 are reliable at only three pH values, minus fumarate, and two pH values, plus fumarate, they suggest that k_{4O_2} and k_5 are constant within experimental error from pH 4.5 to 6.0, consistent with the low pH behavior expected from eq 6 and 7 in Table III. A further increase in pH above 6.0 leads to a clear-cut decrease in both k_{4O_2} and k_5, confirming that $E_{B2}^{B1}\cdot S_1\cdot S_2$ is incompetent either to proceed to product ($k'_5 = 0$) or to dissociate oxygen ($k'_{4O_2} \simeq 0$) as deduced from the pH dependences of $^{D}(V_{max}/K_{DM})$, Figure 3, and k_5/k_{4O_2}, Table V. Overall, the available data support the preferred binding and release of oxygen and turnover of substrate from the enzyme form E_{B2}^{B1H} (dotted box, Scheme II). A notable exception to this pathway involves dopamine binding, and the interaction of dopamine with enzyme is considered in greater detail below.

The observed increase in k_{4DM} from pH 4.5 to 6.0 is well outside the range of propagated error and contrasts with the behavior of k_{4O_2} and k_5. As noted earlier, the pH dependences of $^{D}(V_{max}/K_{DM})$, Figure 3, and the partitioning ratio k_5/k_{4DM}, Table V, indicate a kinetically competent release of dopamine from $E_{B2}^{B1}\cdot S_1\cdot S_2$. From the data in Table VII, we confirm that dopamine undergoes faster dissociation from E_{B2}^{B1} than E_{B2}^{B1H}. Thus, the change in kinetic order to a preferred release of dopamine at pH 6.6 is a consequence of an additional pathway for loss of dopamine at $[H^+] < K_3$.

The role of fumarate in modulating dopamine β-monooxygenase activity is further clarified by the data in Table VII. Little effect of fumarate appears in k_{3DM}, k_{3O_2}, k_{4O_2}, or k_5, following correction for pK shifts, and only a small inhibitory effect is observed on k_7 across the entire pH range, attributed to a direct effect of fumarate on product release. The most dramatic effect of fumarate appears on k_{4DM}, where we estimate a 3-fold decrease at pH 4.5 vs. a 56-fold decrease at pH 6.0.

Table VII: Microscopic Rate Constants as Functions of pH and Fumarate[a]

	pH							
	4.5		5.2	6.0		6.6		6.8
constant	−F	+F	−F	−F	+F	−F	+F	+F
k_{3O_2} ($\times 10^{-5}$ M^{-1} s^{-1})	2.7 ± 0.5	3.0 ± 0.6	2.5 ± 0.3	1.3 ± 0.2	3.9 ± 0.4	0.43 ± 0.10	3.2 ± 1.3	1.4 ± 0.4
k_{3DM} ($\times 10^{-4}$ M^{-1} s^{-1})	1.6 ± 0.1	1.0 ± 0.8	3.7 ± 0.9	3.0 ± 0.7	2.7 ± 0.2	i	1.3 ± 0.09	1.8 ± 0.6
k_{4O_2} (s^{-1})	270 ± 100	190 ± 80	i	820 ± 370	300 ± 55	37 ± 12	i	i
k_{4DM} (s^{-1})	29 ± 28	9.4 ± 12.0	i	1500 ± 700	27 ± 10	i	i	i
k_5 (s^{-1})	430 ± 140	550 ± 180	i	1200 ± 540	580 ± 110	54 ± 15	i	i
k_7 (s^{-1})	61 ± 6	41 ± 3	45 ± 3	18 ± 0.1	13 ± 0.1	9.1 ± 1.3	8.6 ± 0.3	6.4 ± 0.4

[a] Calculated from eq 1-8, Table VI, where $^{D}k = 9.4 \pm 1.3$, plus fumarate, and $^{D}k = 10.9 \pm 1.9$, minus fumarate. Numbers are reported with two significant figures. Indeterminate values indicated as i.

In addition to indicating trends in individual rate constants as a function of pH and fumarate, the data in Table VII allow assignment of values to each microscopic rate constant subsequent to formation of enzyme–substrate binary complexes. We emphasize that the validity of these assignments depends upon the molecular weight employed in converting initial rate parameters to rate constants and the accuracy of the minimal kinetic mechanism. Ambiguity exists as to whether an active site in dopamine β-monooxygenase is formed at the interface of two subunits, M_r 150 000, or on each subunit, M_r 75 000. For our calculations, an active site molecular weight of 75 000 was assumed; if the correct subunit molecular weight is 150 000, each rate constant in Table VII will be increased 2-fold. Northrop (1981) has recently discussed the influence of minimal kinetic mechanisms on the interpretation of isotope effects on V_{max}, demonstrating that reversible precatalytic steps can either increase or decrease the magnitude of observed V_{max} isotope effects. In general, variation in the magnitude of precatalytic steps by several orders of magnitude leads to very small variations in $^{D}(V_{max})$, indicating a minimal impact of precatalytic steps both on $^{D}(V_{max})$ and calculated rate constants.

In summary, calculation of microscopic rate constants supports our mechanism in Scheme II and provides estimates of the absolute magnitudes of the rate constants. Single turnover experiments in progress in our laboratory are expected to provide an independent measure of the microscopic rate constants, for comparison to these values.

Mechanistic Implications. (A) Chemical Mechanism. An important conclusion from this study is that catalysis requires the protonated form of an enzyme-bound residue, pK = 5.6–6.8, suggesting an acid-catalyzed activation of oxygen to generate a reactive intermediate. Subsequent cleavage of the C–H bond at the β-carbon of substrate may be mediated either directly by an intermediate oxygen species or by an active site residue. If the latter mechanism operates, a single residue could function in acid catalysis of oxygen reduction, followed by general base catalysis of the rate-limiting hydrogen abstraction step. Independent of the mechanism of C–H bond cleavage, the available data indicate that *the first of two protons required by the overall equilibrium stoichiometry in eq 1 must enter the catalytic sequence prior to substrate activation.* One reasonable model attributes acid catalysis to the formation of an enzyme-bound Cu(II)–peroxide complex followed by a rate-limiting C–H bond abstraction step:

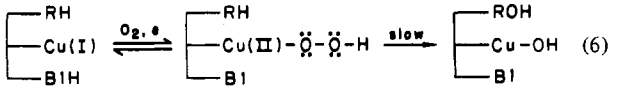

(6)

The pH dependence of product release provides some insight into the role of the second proton. As discussed, product release is facilitated by protonation of a residue with pK = 5.2–5.4; since k_7 decreases only 6-fold between pH 4.0 and 7.0, product dissociation must occur from both E^{B1}_{B2} and E^{B1}_{B2H} with $k'''_7 > k''_7$ (Scheme II). Thus, protonation of EB2 is not essential for enzyme turnover. This residue might influence activity indirectly; we have already noted that the ionization of EB2H appears insensitive to fumarate, in marked contrast to the ionization of the essential (active site) residue EB1H. Alternately, the preferred release of product from E^{B1}_{B2H}·PH may reflect a direct involvement of B2H at the active site. A simple mechanism invokes a proton transfer to an enzyme-bound hydroxide or alkoxide product (illustrated in eq 7 as transfer to hydroxide product):

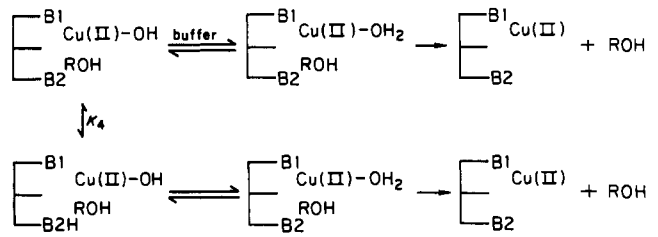

(7)

In this model, the enzyme complex at pH < pK_4 contains fully protonated products, facilitating release of norepinephrine and water. At pH > pK_4, either water or norepinephrine would be ionized and, hence, more tightly bound to the active site. This mechanism provides a logical entry point for the second of two required protons and a good rationale for a preferred rather than obligatory loss of product from E^{B1}_{B2H}, since hydronium ion or buffer could function as proton donor at pH > pK_4. Nevertheless, the validity of eq 7 will depend on the magnitudes of the ionization constants for enzyme-bound products. It is well-known that protein environments can perturb the pKs of ionizable groups far from those observed in solution; for example, inner-sphere coordination to an active site Zn(II) has been proposed to perturb the pK of alcohol to 6.4 in horse liver alcohol dehydrogenase (Kvassman & Pettersson, 1978). In our model for dopamine β-monooxygenase, pK_4 must represent the ionization of the residue with the highest pK, be it donor (EB2H) or acceptor [Cu(II)–OH or Cu(II)–OR]. Since this requires that the pK of metal-bound alkoxide or hydroxide be less than or equal to 5.4, designation of pK_4 to an active site residue must remain speculative at this time.

(B) Anion Activation Mechanism. The data presented in this paper support dual roles for fumarate in the activation

Scheme III: Simple Electrostatic Model Describing Effect of Fumarate on Rate of Dopamine Release from Ternary Substrate Complex and Ionization of B1

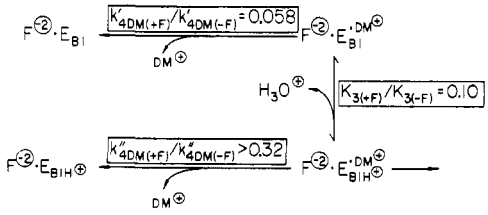

of dopamine β-monooxygenase: (i) a perturbation of pK so that enzyme remains protonated and, hence, optimally active over a wider pH range and (ii) a diminution in the rate of dopamine dissociation leading to an increased steady-state concentration of enzyme ternary complex at nonsaturating dopamine concentrations.

Several lines of evidence have been presented for a perturbation of pK_1 and pK_3, which include the pH dependences of $k_{3\,O_2}$, Figure 4, and $^{D}(V_{max})$, Figure 3. If one assumes that the magnitude of this perturbation is unchanged for the enzyme–dopamine and enzyme–dopamine–oxygen complexes, fumarate can be concluded to reduce K_3 10-fold. Estimation of the effect of fumarate on limiting rate constants for dopamine dissociation from ternary complex is possible from the data in Table VII, when p$K_3 \simeq$ pK_1. The value of $k_{4\,DM}$ between pH 4.5 and 6.0 is expected to vary from $k''_{4\,DM}$ to a sum of $k''_{4\,DM}$ and $k'_{4\,DM}$, depending on the magnitude of $K_3/[H^+]$:

$$k_{4\,DM} = \frac{k''_{4\,DM} + k'_{4\,DM}K_3/[H^+]}{1 + K_3/[H^+]} \qquad (8)$$

At low pH (4.5) in the presence of fumarate, pK_3 = 6.8 is more than 2 pH units above the experimental pH, and we can ascribe $k_{4\,DM}$ to $k''_{4\,DM}$. In the absence of fumarate, pK_3 is reduced to 5.8, and it is no longer possible to neglect the contribution of $k'_{4\,DM}$ to $k_{4\,DM}$. Hence, $k''_{4\,DM}$ (−fumarate) is less than $k_{4\,DM}$, and we conclude that $k''_{4\,DM}$(+fumarate)/$k''_{4\,DM}$(−fumarate) is greater than 0.32. Values for $k'_{4\,DM}$(±fumarate) can be calculated from eq 8 and the pH 6.0 data in Table VII, employing estimates for $k''_{4\,DM}$ and pK_3. Although uncertainty exists regarding $k''_{4\,DM}$(−fumarate), $k'_{4\,DM}$(−fumarate) is insensitive to this constant; i.e., the term $k'_{4\,DM}(K_3/[H^+])$ dominates the numerator in eq 8. Thus we estimate that $k'_{4\,DM}$(+fumarate) = 140, $k'_{4\,DM}$(−fumarate) = 2400, and $k'_{4\,DM}$(+fumarate)/$k'_{4\,DM}$(−fumarate) = 0.058.

These effects of fumarate on dopamine dissociation and K_3 are summarized in Scheme III. Several features emerge from inspection of this scheme. First, the effect of fumarate on the ionization of K_3 is similar to its effect on dopamine dissociation. As noted earlier, the observed pH dependences on V_{max}/K_m are outside the range of pK values for dopamine, and dopamine is expected to bind to dopamine β-monooxygenase in a protonated, positively charged form. If EB1H is also positively charged, loss of either dopamine or a proton from $E_{B1H^+}^{DM^+}$ would reduce positive charge at the enzyme active site, suggesting that electrostatic interactions between fumarate dianion and the cationic centers in $F^{-2}\cdot E_{B1H^+}^{DM^+}$ can account for the observed reductions in K_3 and $k_{4\,DM}$.

Further evidence for an electrostatically induced anion activation is shown by the effect of fumarate on dopamine dissociation above pK_3. As seen in Scheme III, $k_{4\,DM}$(+fumarate)/$k_{4\,DM}$(−fumarate) decreases more than 5.5-fold following ionization of EB1H$^+$ to EB1. If fumarate interactions are solely electrostatic in origin, the energy of stabilization of bound dopamine is expected to increase 2-fold in the $F^{-2}\cdot E_{B1}^{\cdot DM}$ complex. Representing the stabilization energy of bound dopamine by

$$\begin{aligned} \text{pH} < \text{p}K_3\text{:}\quad & E = -RT \ln \frac{k''_{4\,DM}(\text{+fumarate})}{k''_{4\,DM}(\text{−fumarate})} \\ \text{pH} > \text{p}K_3\text{:}\quad & E = -RT \ln \frac{k'_{4\,DM}(\text{+fumarate})}{k'_{4\,DM}(\text{−fumarate})} \end{aligned} \qquad (9)$$

we calculate a value ≥2.5 for the ratio of E(pH > pK_3) to E(pH < pK_3), in reasonable accord with predictions. It appears that a simple electrostatic model adequately describes the observed effects of fumarate on dopamine β-monooxygenase. This conclusion may explain why Craine et al. (1973) were unable to obtain evidence for major conformational changes in dopamine β-monooxygenase in the presence of anion effector. A similar model for the activation of tyrosine hydroxylase by inorganic phosphate anion has been recently published (Vigny & Henry, 1982).

In contrast to this simple electrostatic activation by fumarate, the effect of pH on substrate dissociation from the enzyme ternary complex appears more complicated. We do not yet understand the origin of the *increase* in the rate of dopamine dissociation, concomitant with a decrease in oxygen dissociation above pK_3. If simple electrostatic interactions were operative, we would have predicted a slower rate of dopamine dissociation from EB1 than from EB1H$^+$.

Enzyme inactivation studies employing the histidine-specific reagent diethyl pyrocarbonate (Aunis et al., 1973) led previous investigators to suggest an active site histidine. Assignment of EB1H$^+$ to a protonated histidine residue is consistent with the observed pK = 5.8–6.8. As shown in eq 10, electrostatic interactions between point charges, q_1 and q_2, are inversely proportional to distance:

$$E = \frac{q_1 q_2}{Dr} \qquad (10)$$

where D is the dielectric constant and r is the distance between charges. Thus, the observation of similar effects of fumarate on K_3 and $k_{4\,DM}$ implies a spatial proximity of EB1H$^+$ to dopamine, i.e., a role for histidine at the enzyme active site. Depending on the magnitude of D, a wide range of distances between fumarate and the enzyme active site will satisfy the observed kinetic effects. Independent measurement of distance between dopamine and fumarate bound to dopamine β-monooxygenase would provide further insight into the molecular mechanism of fumarate, as well as a quantitative estimate of the local dielectric constant in the vicinity of the dopamine β-monooxygenase active site.

The putative role of anions in the modulation of enzyme activity in vivo remains unclear. From the present study, which shows a large pH dependence for fumarate activation, anions are unlikely to exert a large stimulatory effect as long as the internal pH of storage vesicles remains ≤5.5. As already discussed, the dopamine β-monooxygenase reaction consumes two protons per turnover; in the event of an imbalance between dopamine β-monooxygenase activity and the ATP-dependent transport of protons and substrate during dopamine turnover, fluctuations in the intravesicular concentrations of dopamine and protons may occur. Under conditions of a decrease in hydrogen ion concentration (below 10^{-5} M) and dopamine concentration (below saturation), the data presented in this paper predict a marked effect of anions on the maintenance of the steady-state concentration of $E_{B1H^+}^{DM^+}$ and, hence, the rate

of norepinephrine production.

Acknowledgments

We thank Dr. Monica Palcic, Chemistry Department, The Ohio State University, for the synthesis and purification of [2-$^2H_2$]dopamine hydrochloride substrate.

Registry No. DM, 51-61-6; [2-$^2H_2$]dopamine hydrochloride, 27160-01-6; (3,4-dimethoxyphenyl)acetonitrile, 93-17-4; 2-(3,4-dimethoxyphenyl)[2-$^2H_2$]ethylamine hydrochloride, 85479-74-9; dopamine β-monooxygenase, 9013-38-1; fumarate, 110-17-8; hydrogen ion, 12408-02-5; deuterium, 7782-39-0.

References

Aunis, D., Miras-Portugal, M. T., & Mandel, P. (1973) *Biochim. Biophys. Acta 327*, 313–327.
Cleland, W. W. (1977) *Adv. Enzymol. Relat. Areas Mol. Biol. 45*, 273–387.
Cleland, W. W. (1979) *Methods Enzymol. 63*, 103–138.
Cook, P. F., & Cleland, W. W. (1981a) *Biochemistry 20*, 1797–1805.
Cook, P. F., & Cleland, W. W. (1981b) *Biochemistry 20*, 1805–1816.
Craine, J. E., Daniels, G. H., & Kaufman, S. (1973) *J. Biol. Chem. 248*, 7838–7844.
Diliberto, E. J., & Allen, P. L. (1981) *J. Biol. Chem. 256*, 3385–3393.
Fersht, A. (1977) *Enzyme Structure and Mechanism*, pp 134–155, W. H. Freeman, San Francisco, CA.
Goldstein, M., Joh, T. H., & Garvey, T. Q., III (1968) *Biochemistry 7*, 2724–2730.
Klinman, J. P., & Krueger, M. (1982) *Biochemistry 21*, 67–75.
Klinman, J. P., Humphries, H., & Voet, J. G. (1980) *J. Biol. Chem. 255*, 11648–11651.
Knowles, J. R. (1976) *CRC Crit. Rev. Biochem. 4*, 165–173.
Kvassman, J., & Pettersson, G. (1978) *Eur. J. Biochem. 87*, 417–427.
Levin, E. Y., Levenberg, B., & Kaufman, S. (1960) *J. Biol. Chem. 235*, 2080–2086.
May, S. W., Phillips, R. S., Mueller, P. W., & Herman, H. H. (1981) *J. Biol. Chem. 256*, 8470–8475.
Miller, S. M., & Klinman, J. P. (1982) *Methods Enzymol. 87*, 711–732.
Miller, S. M., & Klinman, J. P. (1983) *Biochemistry* (preceding paper in this issue).
Miras-Portugal, M. T., Aunis, D., & Mandel, P. (1973) *FEBS Lett. 34*, 140–142.
Njus, D., & Radda, G. K. (1978) *Biochim. Biophys. Acta 463*, 219–244.
Northrop, D. B. (1981) *Biochemistry 20*, 4056–4061.
Rosenberg, R. C., & Lovenberg, W. (1980) *Essays Neurochem. Neuropharmacol. 4*, 163–209.
Skotland, T., & Ljones, T. (1979a) *Inorg. Perspect. Biol. Med. 2*, 151–180.
Skotland, T., & Ljones, T. (1979b) *Eur. J. Biochem. 94*, 145–151.
Skotland, T., & Ljones, T. (1980) *Biochim. Biophys. Acta 630*, 30–35.
Terland, O., & Flatmark, T. (1975) *FEBS Lett. 59*, 52–56.
Vigny, A., & Henry, J. P. (1982) *Biochem. Biophys. Res. Commun. 106*, 1–7.
Villafranca, J. J. (1981) *Met. Ions Biol. 3*, 263–289.
Von Euler, U. S., & Floding, I. (1955) *Acta Physiol. Scand., Suppl. No. 118*, 45–56.

Polypeptide Clearing in Model Membranes: An Analysis of the Partition of Gramicidin A′ between Cadmium Ion Induced Gel and Liquid-Crystalline Phases in Vesicles of Phosphatidic Acid and Phosphatidylcholine†

Gerald W. Feigenson

ABSTRACT: Using a simple model for a biological membrane we examine cation-induced gel phase formation and the depletion of polypeptide from the gel phase. The model system consists of vesicles of phosphatidic acid and phosphatidylcholine which contain gramicidin A′. By use of electron spin resonance to monitor lipid phase behavior, Cd^{2+} is found to induce gel and liquid-crystal phase coexistence over a wide range of lipid composition. Quenching of gramicidin A′ tryptophanyl fluorescence by spin-labeled phosphatidic acid or spin-labeled phosphatidylcholine is analyzed to obtain the partition coefficient, K_p, for gramicidin A′ between gel and liquid-crystal phases. The value of $K_p = 3$ favoring the liquid-crystal phase indicates a partial clearing of the membrane-bound polypeptide from Cd^{2+}-induced gel phase regions of the membrane.

Electron microscopy of fusing biological membranes utilizing fixed and stained thin sections and cryoprotected freeze–fracture has revealed membrane regions in contact to be relatively free of protein (Chi et al., 1979; Lawson et al., 1977; Orci et al., 1977; Peixoto de Menezes & Pinto da Silva, 1978; Kalderon & Gilula, 1979). This finding has been disputed by workers using rapidly frozen membrane samples without cryoprotectant (Chandler & Heuser, 1979, 1980; Ornberg & Reese, 1981). These latter studies suggest that the regions of initial contact of fusing membranes are probably too small in area to allow detection of the putative clearing of intramembrane particles. Freeze–fracture electron microscopy of reconstituted model membranes containing Ca^{2+} ATPase from sarcoplasmic reticulum (Kleemann & McConnell, 1976) or glycophorin (Grant & McConnell, 1974) showed particle-free regions thought to correspond to patches of

† From the Section of Biochemistry, Molecular and Cell Biology, Clark Hall, Cornell University, Ithaca, New York 14853. *Received November 10, 1982.* This work was supported by a grant from the National Institutes of Health, U.S. Public Health Service (HL-18255). This work was done during the tenure of an Established Investigatorship of the American Heart Association.

0006-2960/83/0422-3106$01.50/0 © 1983 American Chemical Society